Hindawi Publishing Corporation
Journal of Renewable Energy
Volume 2014, Article ID 624502, 8 pages
http://dx.doi.org/10.1155/2014/624502

Research Article

Design and Modelling of Water Chilling Production System by the Combined Effects of Evaporation and Night Sky Radiation

Ahmed Y. Taha Al-Zubaydi and W. John Dartnall

School of Electrical, Mechanical & Mechatronic Systems, University of Technology Sydney, 15 Broadway, Ultimo, NSW 2007, Australia

Correspondence should be addressed to Ahmed Y. Taha Al-Zubaydi; ahmedyassintaha@hotmail.com

Received 24 September 2013; Accepted 2 January 2014; Published 2 March 2014

Academic Editor: Czarena Crofcheck

The design and mathematical modelling of thermal radiator panel to be used primarily to measure night sky radiation wet coated surface is presented in this paper. The panel consists of an upper dry surface coated aluminium sheet laminated to an ethylene vinyl acetate foam backing block as an insulation. Water is sprayed onto the surface of the panel so that an evaporative cooling effect is gained in addition to the radiation effect; the surface of a panel then is wetted in order to study and measure the night sky radiation from the panel wet surface. In this case, the measuring water is circulated over the upper face of this panel during night time. Initial TRNSYS simulations for the performance of the system are presented and it is planned to use the panel as calibrated instruments for discriminating between the cooling effects of night sky radiation and evaporation.

1. Introduction

The demand for energy efficient air conditioning systems to minimize the energy consumption worldwide has been an important issue for researchers since the invention of active air conditioning system. In parallel with the researches conducted to create new conventional air conditioning technologies, researches to find noncompressor systems took a place.

Noncompressor cooling systems have been introduced as low electricity consumption alternatives to mechanical vapour compression units, providing a solution that reduces the energy consumption and environmental issues in buildings. Absorption and adsorption chillers, direct and indirect evaporative air coolers, and water passive cooling systems which utilize the night sky radiation effect are among the range of noncompressor systems available. Radiative cooling is a passive cooling process based on the phenomenon of heat transfer between earth-based objects and the sky by the means of long-wave radiation, usually when the effective sky temperature is less than the ground temperature. The transparency of earth's atmosphere in the infrared range of 8–13 μm (atmospheric window) allows a fraction of the thermal radiation to be absorbed by space, especially during the night and early morning where solar short wave radiation is absent. The phenomenon can be applied to cool surfaces and/or fluids, which in turn can be used in air conditioning applications.

Cooling with night sky radiation phenomena could be considered as featured technology with capability to be a passive alternative to the conventional air conditioning system. Many researchers have explored the different applications and systems proposed to cool fluids by means of heat rejection by radiation to the sky. Yannas et al. [1] presented the world's best-known applications of the night sky radiation system with mathematical modelling of a roof pond system. Spanaki [2] presented a comparison between different roof pond systems for cooling. Tiwari et al. [3] presented the analysis of the moving water system in three different cases including roof pond, spray cooling/gunny bags, and moving water over the roof.

A commercial system known as "WhiteCap" was introduced in the United States. This system is reported by Bourne and Carew [4, 5]. The WhiteCap system employs the cooling of water by night sky radiation, convection, and evaporation of water in an open water cycle. The cold water is stored for use during the day by direct conduction to the roof (WhiteCap-R), fan coils (WhiteCap-T), or coils entrenched in the floor slab (WhiteCap-F). The WhiteCap system enhances

the evaporation heat loss by spraying the water over the roof in the primary stage, and the water droplets evaporate as they travel from the spray outlet to the roof surface. Bourne and Carew [4] reported a 47% reduction in annual use of conventional cooling by using the WhiteCap cooling system on a 2,500-square-meter office building in Los Angeles.

The low cooling capacity and the high effectiveness of ambient conditions on the system performance (i.e., cloud cover and relative humidity) are considered practical limitations of the nocturnal cooling by radiation technology applications. However, the system can be applied as a supplemental heat sink system with another HVAC system [6]. Examples of hybrid systems are presented by Heidarinejad et al. [7] and Farmahini Farahani et al. [8]. Both studies investigated the possible combination of nocturnal radiation cooling systems with conventional systems, specifically with an indirect evaporative cooling unit in the first study and a direct evaporative cooling unit in the second.

Although the WhiteCap system is available since 1996, no theoretical works available present the system mathematical modelling. In previous work, the author presented a mathematical modelling of three different systems applying the Night sky radiation for water chilling [9]. The system compared three panels to measure the various effects: the first panel had a dry radiative surface with an embedded heat exchange water circuit for the purpose of measuring the radiant heat. The second panel employed a sprayed water flowing over its radiative surface to measure combined effect of (a) heat lost by pre-evaporation during the sprayed water droplet travel through the air, (b) evaporation of water flowed over the radiation surface and (c) radiation from the thin water layer surface. The third panel is like the second, however the water is running via a gutter at the top so that is flows over the radiative surface enables the heat loss by radiation and evaporation from a wetted surface. The comparison between the three systems shows that the second panel performance is the best in term of water chilling.

In this work, the author presented the second system presented in the previous work [9] with a detailed mathematical modelling to enable researchers to use it as a design guide for future work. In order to satisfy the above objective, it was decided to construct a panel having similar principles of the WhiteCap system. By using this panel, the separate effects of evaporative cooling and night sky radiative cooling may be deduced from the recorded data. In this work we discussed the design and mathematical modelling of the system (i.e., radiator panel with sprayer). The system under investigation is described in Figure 1. The layout of the system (Figure 1) consists of a radiator panel with a well-insulated back side which is used to simulate the principles of the system similar to the WhiteCap system. Water is sprayed onto the panel flow for a measured distance and then returned to the storage tank and pumped again. The contact of the water with the air causes mass loss by the evaporation through the process; make-up water to the tank is a necessity. The make-up water temperature is different from the water temperature in the storage tank, and this is considered in the calculations. The water temperatures in the tank, spray nozzle inlet, water pond inlet, and water pond outlet are the data collected.

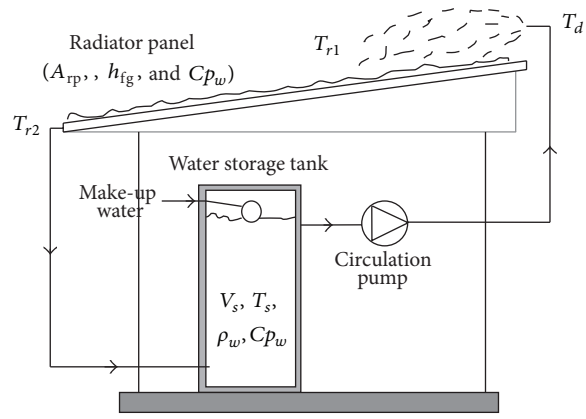

Figure 1: Experimental setup for the radiative cooling measurement systems-radiator panel with sprayer.

This paper discusses the theoretical work of the project by presenting mathematical modelling and a performance simulation with the Transient System Simulation Tool (TRNSYS) software package [9, 10]. The results are analysed to optimize the design parameters and to analyse the contribution of the three heat transfer phenomena that occur in different applications of cooling water using the night sky radiation effect. We also study the feasibility of producing chilled water for space cooling applications. The simulation results will be analysed and compared with the experimental results in a later stage of the project.

2. System Description and Modelling

2.1. The Effective Sky Temperature. The heat exchange between the radiator plate and the sky occurs in a wavelength range of 8 to 14 μm, or what is known as the atmospheric window. The sky is considered to be a black body of equivalent temperature T_{sky} or the effective sky temperature. In the literature [11–13], many equations have been introduced to calculate T_{sky}, as a function of the ambient temperature, cloudiness factor, and the emissivity of the clear sky which in turn is a function of ambient temperature, relative humidity, and atmospheric pressure. Berdahl and Martin [11, 13] introduced an equation to calculate the clear sky emissivity as follows:

$$\varepsilon_{sky} = 0.711 + 0.005T_{dp} + 7.3 \times 10^{-5}T_{dp}^2 + 0.013\cos\left[2\pi\frac{\text{time}}{24}\right] + 12 \times 10^{-5}\left(P_{atm} - P_h\right), \quad (1)$$

where T_{dp} is the dew point temperature (°C), P_{atm} is the atmospheric pressure (atm), P_h is the atmospheric pressure at elevation h (m) above sea level, and the variable (time) is the hour of the day. In the TRNSYS software package, the Type 69 calculates the effective sky temperature T_{sky} (K) using Martin and Berdahl's [13] equation as follows:

$$T_{sky} = T_{amb}\left(\varepsilon_{sky} + 0.8\left(1 - \varepsilon_{sky}\right)C_{clo}\right)^{1/4}, \quad (2)$$

where C_{clo} is the sky cloudiness factor (0-1), supplied by TRNSYS Type 69.

2.2. Thermal Panel Description. A thermal panel for the purpose of cooling water with night sky radiation was designed using basic materials which cost little and make the labour easier. The assembly consisted of an aluminium plate with dimensions of 3000 mm long, 2000 mm wide, and 2 mm thick. The dimensions were chosen to fit the size of a piece of EVA foam supplied directly by the manufacturer. The plate was fixed to a 30 mm thick EVA foam block of closed cell foam made from ethylene vinyl acetate and blended copolymers. In the open cycle water system, water is sprayed over the roof surface and flows onto the low, sloped surface for a distance of L (m) before being collected and returned to the tank. The operation is repeated during the night (Figure 1). Water exchanges heat with the ambient air by means of evaporation and convection and to the sky by radiation. The relative temperature of the water in the tank will be changed by the end of the operating period. In the following the modelling of each process is presented.

2.2.1. Water Droplet Modelling. In this section, the calculation of the sprayer water droplet final temperature and the quantity of evaporative mass will be discussed. The modelling of water droplet energy balance has been presented earlier by Al-Zubaydi et al. [9]. A numerous number of water droplets formed by the nozzle will travel through the air to the water pond on the panel surface, performing a heat and mass transfer with the surrounding air. The process is assumed to be a quasisteady state that varies with the ambient temperature in the form of Fourier series. The water droplet boundary system energy balance is presented in Figure 2 [14]. The quantity of heat stored in the droplets over the period of time Δt is

$$\Delta \dot{U} = \dot{Q}_{\text{total}}. \tag{3}$$

The internal energy of the system is calculated by

$$\Delta \dot{U} = m_d \cdot C_{pw} \cdot \frac{\Delta T_d}{\Delta t}, \tag{4}$$

where m_d is the mass of the droplet (kg), C_{pw} is the specific heat capacity of the water (J/kg·K), and ΔT_d is the difference between the droplet final temperature T_{d2} and initial temperature T_{d1} (K).

The heat transfer between the droplets, the surroundings, and the ambient air is the sum of all heat transfers by convection, radiation, evaporation, and condensation.

Essentially, when evaporation occurs, no condensation takes part in the thermodynamic process and the value of heat transfer by condensation is reset to zero. The total heat transfer from a droplet boundary system is given by

$$\dot{Q}_{\text{total}} = \dot{Q}_{\text{conv}} + \dot{Q}_{\text{rad}} - \dot{Q}_{\text{evap}}, \tag{5}$$

where

$$\dot{Q}_{\text{conv}} = h_{\text{conv}} \cdot A_d \cdot \left(T_{\text{amb}} - T_d\right), \tag{6}$$

$$\dot{Q}_{\text{rad}} = \varepsilon_{\text{water}} \cdot A_d \cdot \sigma \cdot \left(T_{\text{sky}}^4 - T_d^4\right), \tag{7}$$

$$\dot{Q}_{\text{evap}} = \dot{m}_{\text{evap}} \cdot h_{fg}, \tag{8}$$

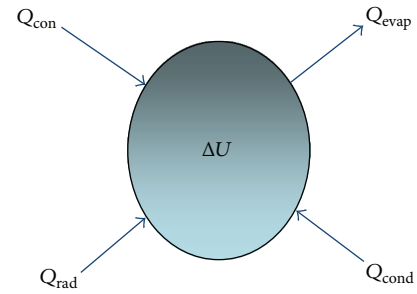

Figure 2: Water droplet energy balance.

where h_{conv} is the coefficient of thermal convection (w/m^2·K) and h_{fg} is the evaporation enthalpy of water vapor (J/kg). A_d is the surface area of the droplet (m^2), m_d is the single droplet mass (kg), σ is the Stefan-Boltzmann constant (5.67×10^{-8} w/m$^2 \cdot$ K^4), and $\varepsilon_{\text{water}}$ is the water surface emissivity (value set to 1). By substituting (9)–(13) in (8) and rearranging we get

$$T_{d2} = T_{d1} + \frac{\Delta t}{m_d \cdot C_{pw}} \times \left[h_c \cdot A_d \cdot \left(T_a - T_d\right) + \varepsilon_{\text{water}} \cdot A_d \cdot \sigma \cdot \left(T_{\text{sky}}^4 - T_d^4\right) - \dot{m}_{\text{evap}} \cdot h_{fg}\right], \tag{9}$$

where T_{d2} is the water drop final temperature (K) and T_{d1} is the water droplet initial temperature (K). h_c and $\dot{m}_{\text{evap}}$ values can be calculated with the following equations, the mass evaporation rate $\dot{m}_{\text{evap}}$ (kg/s):

$$\dot{m}_{\text{evap}} = h_m \cdot A_d \cdot \left[\rho_{\text{drop}} - \phi \rho_{\text{atm}}\right], \tag{10}$$

where h_m is the mass transfer convection coefficient (m/s), ρ_d is the specific humidity of saturated air evaluated at the water droplet temperature (kg/m^3), ρ_{amb} is the specific humidity of saturated air evaluated at the ambient temperature (kg/m^3), and φ is the relative humidity of the ambient air (%).

h_m is derived from the Sherwood number [14]:

$$\text{Sh}'_D = 2 + 0.6\text{Sc}^{1/3}\text{Re}^{1/2}, \tag{11}$$

where Re is the Reynolds number of the droplet and is given by

$$\text{Re} = \frac{D_d s_d}{\nu_{\text{air}}}, \tag{12}$$

where D_d is the droplet diameter (m), s_d is the droplet velocity (m/s), and ν_{air} is the kinematic viscosity for air (m^2/s). The variable Sc is the Schmidt number and is given by

$$\text{Sc} = \frac{\nu_{\text{air}}}{D_{\text{vap}}}, \tag{13}$$

where D_{vap} is the water vapour diffusivity in air (m^2/s) [0.26E−4 m^2/s] [15]. After calculating the Sherwood number, the value of h_m is given by

$$h_m = \frac{\text{Sh}'_D \cdot D_{\text{vap}}}{D}. \tag{14}$$

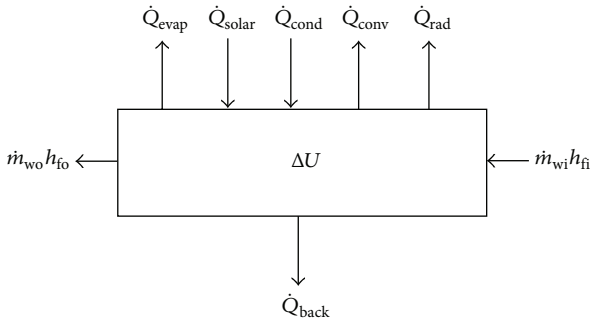

Figure 3: Water pond energy balance.

The coefficient of thermal convection h_c can be derived from the Nusselt number equation:

$$\mathrm{Nu} = \frac{h_{\mathrm{conv}} D_d}{k_{\mathrm{air}}}, \tag{15}$$

where k_{air} is the air thermal conductivity (W/m·k). In forced convection between the droplet and the wind, the Nusselt number can be calculated by the Ranz and Marshal [15] equation:

$$\mathrm{Nu} = 2 + 0.6\mathrm{Pr}^{1/3}\mathrm{Re}^{1/2}. \tag{16}$$

The Prandtl number Pr can be found in the air properties table or calculated as a function of air dynamic viscosity ν_a, specific heat of the air C_{pa}, and air thermal conductivity k_{air}, with formula [16]:

$$\mathrm{Pr} = \frac{C_{pa}\nu_a}{k_{\mathrm{air}}}. \tag{17}$$

By substituting the outputs of (11) and (16) in (15), the substitute equation (15) output in (14), the value of h_{conv} will be

$$h_{\mathrm{conv}} = \frac{k_{\mathrm{air}}\left[2 + 0.6\mathrm{Pr}^{1/3}\mathrm{Re}^{1/2}\right]}{D_d}. \tag{18}$$

With the values of h_c and $\dot{m}_{\mathrm{evap}}$ calculated from (16) to (24), the new temperature of the droplet T_{d2} can be estimated; this temperature will be the initial temperature of the second part of the water cooling system, the panel pond. The amount of water entering the water pond boundary system is the initial mass flow rate of the sprayer minus the evaporated losses:

$$m_{2s} = m_{1s} - \left(\dot{m}_d \cdot \Delta t \cdot \frac{m_{1s}}{m_d}\right). \tag{19}$$

2.2.2. Radiative Panel Mathematical Modelling. Similar to the water droplet, the panel pond control volume can be represented as a typical thermodynamic control volume (Figure 3). As can be seen, the heat transfer to and from the system boundary is in the form of evaporation, conduction, convection, solar, and radiation, in addition to heat transfer due to water entering and leaving the system.

Similar to the water droplet energy equation, the water pond energy equation is

$$m_{w\_\mathrm{rp}} \cdot C_{pw} \cdot \frac{T_{\mathrm{rp2}} - T_{\mathrm{rp1}}}{\Delta t} = \dot{Q}_{\mathrm{cond}} + \dot{Q}_{\mathrm{solar}} - \dot{Q}_{\mathrm{conv}} - \dot{Q}_{\mathrm{rad\_sky}} - \dot{Q}_{\mathrm{evap}} - \dot{Q}_{\mathrm{back}} + \dot{E}_{\mathrm{wi}} - \dot{E}_{\mathrm{wo}}, \tag{20}$$

where m_{w_rp} is the mass of the water in the water pond (kg), $\dot{Q}_{\mathrm{cond}}$ is the heat added by condensed water (kJ/s), $\dot{Q}_{\mathrm{Solar}}$ is the heat absorbed by the panel water pond due to solar radiation (kJ/s), $\dot{Q}_{\mathrm{conv}}$ is the heat convection between the water pond and ambient air (kJ/s), $\dot{Q}_{\mathrm{rad\_sky}}$ is the heat exchange between the water in the roof pond and the sky, by radiation (kJ/s), $\dot{Q}_{\mathrm{evap}}$ is the evaporation heat exchange between water and the ambient air (kJ/s), $\dot{Q}_{\mathrm{back}}$ is the heat transfer between the water and the ambient air through the panel layers (kJ/s), and $\dot{E}_{\mathrm{wi}}$ and $\dot{E}_{\mathrm{wo}}$ are the energy rates added to the panel pond water by the water added and water leaving the system boundary (kJ/s).

As in (3) for the water droplet, the energy equation can be rewritten to calculate the temperature of the water leaving the panel pond:

$$T_{\mathrm{rp2}} = T_{\mathrm{rp1}} + \frac{\Delta t}{m_{w\_\mathrm{rp}} \cdot C_{pw}} \cdot \left[\dot{Q}_{\mathrm{cond}} + \dot{Q}_{\mathrm{solar}} - \dot{Q}_{\mathrm{conv}} - \dot{Q}_{\mathrm{rad\_sky}} - \dot{Q}_{\mathrm{evap}} - \dot{Q}_{\mathrm{back}} + \dot{E}_{\mathrm{wi}} - \dot{E}_{\mathrm{wo}}\right]. \tag{21}$$

Calculations of heat and energy transfers between the system and the boundary can be derivatives using the basic heat transfer equation; many works presenting the mathematical modelling of the panel pond system can also be referenced [17–22]. The amount of heat dissipated to the sky by radiation is a function of the pond emissivity, the sky temperature, and the pond water temperature; other factors having an effect are the humidity ratio, clouds, and radiation wavelength which have a direct effect on changes to the emissivity and sky temperature values. The $\dot{Q}_{\mathrm{rad\_sky}}$ is given by

$$\dot{Q}_{\mathrm{rad\_sky}} = h_{\mathrm{rad\_sky}} \cdot A_{\mathrm{rp}} \cdot \left(T_{w\_\mathrm{rp}} - T_{\mathrm{sky}}\right), \tag{22}$$

where $h_{\mathrm{rad\_sky}}$ is the sky radiation heat transfer coefficient (W/m^2·k), A_{rp} is the panel surface area (m^2), T_{w_rp} is the temperature of the water in the pond (K), and T_{sky} is the effective sky temperature (K).

During the day, solar heat is added to water in the pond area; the amount of heat added depends on the amount of solar irradiation flux (I_{solar}) and the panel pond's solar absorptivity (α_{solar}). The heat absorbed by water from solar irradiation is given by

$$\dot{Q}_{\mathrm{solar}} = \alpha_{\mathrm{solar}} A_{\mathrm{rp}} I_{\mathrm{solar}}. \tag{23}$$

Consider that $\dot{Q}_{\text{conv}}$ is the heat transfer from water to the ambient by convection; this heat can be calculated by

$$\dot{Q}_{\text{conv}} = h_{\text{rp\_conv}} A_{\text{rp}} \left(T_{\text{rp}} - T_{\text{amb}}\right). \quad (24)$$

The convection heat transfer coefficient ($h_{\text{rp\_conv}}$) is a function of the type of flow rate, laminar flow, or turbulent flow, and the ($h_{\text{rp\_conv}}$) general equation is

$$h_{\text{rp\_conv}} = \text{Nu}_L \cdot \frac{K_{\text{amb}}}{X_{\text{rp}}}, \quad (25)$$

where K_{amb} and X_{rp} are the thermal conductivity of the ambient air and the distance water flows over the panel, while Nu_L is the Nusselt number, which is dissimilar to the water droplet (10); in the case of panel pond flow, its value depends on the nature of convection (forced or natural) [16]. The water mass evaporation rate from panel pond $\dot{m}_{\text{rp\_evap}}$ needs to estimate the value of heat dissipated from water by evaporation. By recalling (4) and replacing the droplet surface area by the panel surface area we get

$$\dot{m}_{\text{rp\_evap}} = h_{m\_\text{rp}} \cdot A_{\text{rp}} \cdot \left[\rho_{w\_\text{rp}} - \rho_{\text{atm}}\right], \quad (26)$$

where ρ_{w_rp} and ρ_{atm} are the water density at saturation temperature pressure and atmospheric pressure, respectively (kg/m^3), h_{m_rp} (m/s), the mass transfer coefficient is calculated from the Sherwood number (Sh'_X), and the binary mass diffusion coefficient (D_{vap}) is calculated as

$$h_{m\_\text{rp}} = \frac{\text{Sh}'_X D_{\text{vap}}}{X_{\text{rp}}}. \quad (27)$$

Under forced convection conditions, the Sherwood number is

$$\text{Sh}'_X = 0.644 \text{Re}_X^{1/2} \text{Sc}^{1/3} \quad (28)$$

and the Nusselt number is

$$\text{Nu}_X = 0.644 \text{Re}_X^{1/2} \text{Pr}^{1/3}. \quad (29)$$

When the value of $\dot{m}_{\text{rp\_evap}}$ is calculated with (27), value above zero indicates that evaporation has taken place, and the heat transferred by evaporation from the water to the atmosphere is

$$\dot{Q}_{\text{evap}} = h_g \cdot \dot{m}_{\text{rp\_evap}}. \quad (30)$$

The energy of water entering and exiting from the system boundary (ΔE_w) is

$$\Delta E_w = h_{f,\text{wi}} \dot{m}_{\text{wi}} - h_{f,\text{wo}} \dot{m}_{\text{wo}}. \quad (31)$$

The $h_{f,\text{wi}}$ and $h_{f,\text{wo}}$ are the enthalpies of water entering and exiting the pond, and $\dot{m}_{\text{wi}}$, $\dot{m}_{\text{wo}}$ are the mass flow rate of water entering pond. The $\dot{m}_{\text{wo}}$ is estimated to be the entering water mass flow rate after subtracting the evaporating mass rate.

The heat transfer through the back of the panel ($\dot{Q}_{\text{back}}$) is a function of the back material thermal conductivity and is given by

$$\dot{Q}_{\text{back}} = h_{b_{\text{rp}}} A_{\text{rp}} \left(T_{\text{w\_rp}} - T_b\right), \quad (32)$$

where T_b is the back layer temperature. The h_{b_rp} is the heat transfer coefficient between the back layer and the pond water:

$$h_{b\_\text{rp}} = \frac{K_{\text{plate}}}{dx_{\text{plate}}} + \frac{K_{\text{foam}}}{dx_{\text{foam}}}. \quad (33)$$

Two identical panels with the dimensions of 2400 mm long and 900 mm wide were constructed from aluminum sheets insulated from the bottom to eliminate the heat transfer from the back side. The criteria that determined the panel size included the aim to make a portable prototype and to minimize the labor. As planned, the water will flow over the inclined panels during the night and will be presprayed in one case to evaluate the contribution of water spray over the panel.

3. Results and Discussion

Results presented in the following section are based on the simulation performance of the described system with TRNSYS software package, the standard weather data file TMY2, based on Australian weather data in summer (28/29 January) and on the following input data for the systems:

(i) total panel area for wet surface Aws = 6.00 m^2. Water Tank Volume VT = 250 L.

In the simulation, the panel is treated as a roof sloped by 30° facing south. The simulation performed in two different locations in Australia, that is, Sydney (humid weather) and Alice Spring (hot and dry area).

The system cold water temperature variation during the assigned simulation period from 21:00 hours to 6:00 hours in the following morning is plotted in Figure 4. The pump water flow rate varied in several simulation runs to optimize the system performance; the results show that the temperature in the tank dropped to 11.8°C by the end of the period in the clear night arid conditions of Alice Springs, using the open cycle system with sprayer. However, the high relative humidity rates in Sydney compared to Alice Springs (Figure 6) resulted in a less cooling rate in the water as shown in Figure 5. That is mainly related to the reduction of the heat transfer by evaporation (Q evap) from both drop and water layer.

The convective heat transfer coefficient value from (6) and (24) is proportional to the wind velocity. Analysis of wind velocity data (Figure 7) against the storage tank water temperature in Figures 4 and 5 indicates that the convection effect added heat to the water, thus minimizing the cooling process by radiation. The cloudiness factor (C_{clo}) for the selected day did not exceed 0.19 on average in Sydney and 0.02 in Alice Springs; thus the negative effect of clouds was eliminated. The analysis of the simulation results, built on a simulation

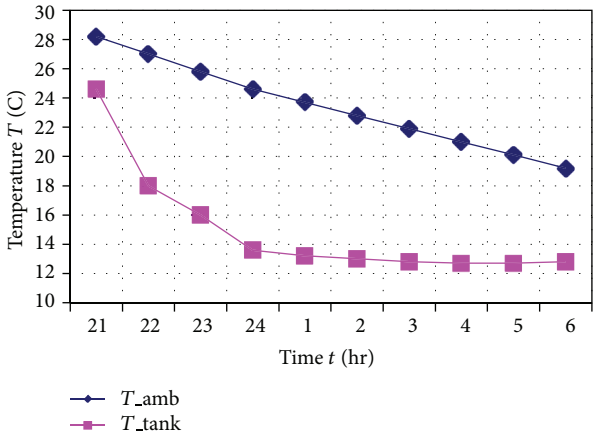

Figure 4: Water cooling with nocturnal cooling effect in Alice Springs using the system described in this work.

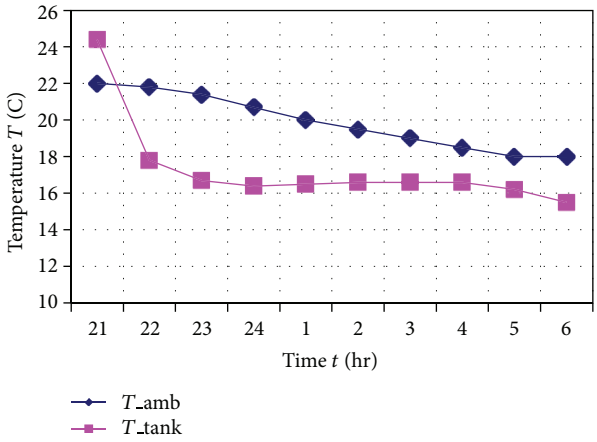

Figure 5: Water cooling with nocturnal cooling effect in Sydney using the system described in this work.

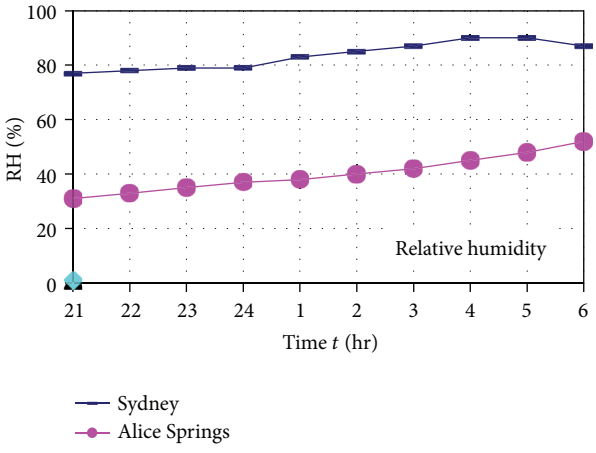

Figure 6: Relative humidity rate in the two locations.

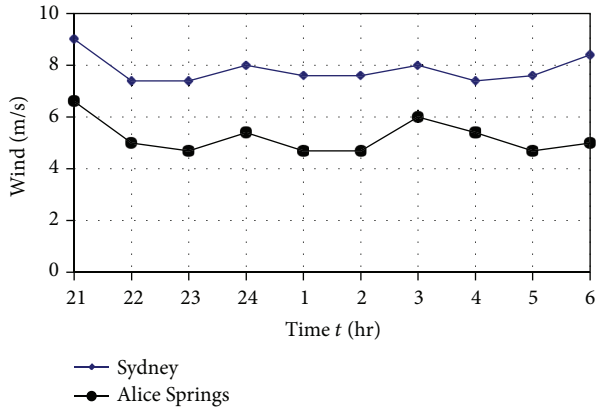

Figure 7: Wind velocity in the four locations.

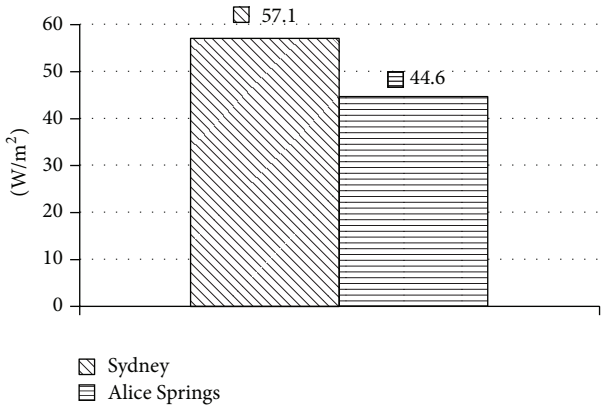

Figure 8: Net sky radiation in two different geographical locations.

time step of 10 seconds, indicates that the system recorded higher net sky radiation value in Sydney than that in Alice Spring (Figure 8). This is strongly related to the absence of the high evaporation rate of water where the water temperature has dropped to a lower value and reduced the temperature difference between the water and the sky temperature (used in (7) and (22)).

The net long wave radiations from the radiator panel in the 2 selected locations are 59.2 W/m^2 in Sydney and around 47 W/m^2 in Alice Springs (Figure 8) calculated from (7) and (23). Although the relative humidity in Alice Springs is lower than in Sydney, the effect of the higher ambient temperature in Alice Springs reduced the rate of the net sky radiation rate.

The storage tank water temperature in both cases was set to a start temperature of 25°C. Lower start-up temperature resulted in lower storage tank final temperature. For example, in Alice Spring weather, a start temperature of 22°C resulted in final temperatures that were 2.5°C lower than this for a start temperature of 25°C. But the results show that, even under unfavourable conditions, the systems have the capacity to cover a fraction of the cooling demand. Generally, the simulations indicate that sufficient radiative cooling is obtained in periods with modest or above air humidity and ambient night temperatures, cooling below 20°C in most cases.

4. Conclusion

In this research, a brief literature review of several researches covering the phenomenon of long wave radiation to the sky was presented. The thermal behaviour of a system utilizing this technology was described by a detailed mathematical modelling. These models simulated different climatic conditions. The simulation results specify that the net long wave radiation to a clear sky on an Australian summer night is sufficient to cool the water in a storage tank with a total volume of 260 litres to low temperature (as low as to 13 degrees lower than the starting temperature of 25°C). The mathematical modelling and simulation results will be used in future research to set up experimental prototype systems to validate the simulation results.

Nomenclature

A_d: Water droplet surface area (m^2)
A_{rp}: Panel surface area (m^2)
C_{clo}: Sky cloudiness factor (—)
C_{pw}: Specific heat capacity of the water (J/kg K)
C_{pw}: Fluid specific heat capacity (J/kg·°C)
D: Droplet diameter (m)
D_{vap}: Binary mass diffusion coefficient (m^2/s)
$\dot{E}_{wi}$: Energy added to pond system boundary (kJ/s)
$\dot{E}_{wo}$: Energy leaving pond system boundary (kJ/s)
h_{conv}: Convective heat transfer coefficient ($W/m^2 \cdot °C$)
h_{m_rp}: The mass transfer coefficient (kg/s)
h_{fg}: Evaporation enthalpy of water vapor (J/kg)
h_{rad_sky}: Sky radiation heat transfer coefficient (W/m^2·k)
h_{rp_conv}: Convection heat transfer coefficient (W/m^2·K)
h_{rad}: Radiative heat transfer coefficient ($W/m^2 \cdot °C$)
I_{solar}: Solar irradiation flux (W/m^2)
K_{amb}: Ambient air thermal conductivity (W/m·K)
K: Thermal conductivity of material (W/m^2·K)
m_d: Mass of the water droplet (kg)
$\dot{m}_{evap}$: Water droplet mass evaporation rate (kg/s)
m_{w_rp}: Mass of the water in the roof pond (kg)
$\dot{m}_{rp\_evap}$: Mass evaporation rate (roof pond) (kg/s)
Nu_L: Nusselt number (—)
n: Number of parallel channels in radiator (—)
P_{atm}: Atmospheric pressure (atm)
P_h: Atmospheric pressure at elevation h (atm)
Q_c: Convection specific heat transfer (W/m^2)
$\dot{Q}_{cond}$: The heat added by condensed water
$\dot{Q}_{Solar}$: Heat due to solar radiation (kJ/s)
$\dot{Q}_{conv}$: Convection heat transfer (kJ/s)
$\dot{Q}_{rad\_sky}$: Radiation heat transfer (kJ/s) (kJ/s)
$\dot{Q}_{evap}$: Evaporation heat transfer (kJ/s)
$\dot{Q}_{back}$: Heat transfer rate from radiator back (kJ/s)
Q_{rad}: Radiative heat exchange (W)
Re_X: Reynolds number (—)
Sh'_X: Sherwood number (—)
T_{amb}: Ambient temperature (°C)
T_{dp}: Dew point temperature (°C)
T_{d1}: Droplet initial temperature (K)
T_{d2}: Droplet final temperature (K)
T_{sky}: Effective sky temperature (K)
T_{w_rp}: Temperature of the water in the pond (K)
U_b: Heat loss coefficients of the panel back ($W/m^2 \cdot °C$)
U_p: Heat loss coefficients of the panel front ($W/m^2 \cdot °C$)
U_r: Radiator overall heat loss coefficient ($W/m^2 \cdot °C$)
V_w: Wind velocity (m/s)
X_{rp}: Distance of water flow over the roof pond (m)
ε_{rad}: The emissivity of radiator plate (—)
$\triangle T_d$: $= (T_{d2} - T_{d1})$ (K)
ε_{water}: Water surface emissivity (—)
α_{solar}: Roof pond solar absorbing (—)
σ: Stefan-Boltzmann constant ($W/m^2 \cdot K^4$).

Conflict of Interests

The authors declare that there is no conflict of interests regarding the publication of this paper.

References

[1] S. Yannas, E. Erell, and J. L. Molina, *Roof Cooling Techniques: A Design Handbook*, Earthscan, London, UK, 2006.

[2] A. Spanaki, "Comparative studies on different type of roof ponds for cooling purposes: literature review," in *Proceedings of the 2nd PALENC Conference and 28th AIVC Conference on Building Low Energy Cooling and Advanced Ventilation Technologies in the 21st Century*, Crete, Greece, September 2007.

[3] G. N. Tiwari, A. Kumar, and M. S. Sodha, "A review—cooling by water evaporation over roof," *Energy Conversion and Management*, vol. 22, no. 2, pp. 143–153, 1982.

[4] R. C. Bourne and C. Carew, "Design and implementation of a night roof-spray storage cooling system," in *Proceedings of the ACEEE Summer Study on Energy Efficiency in Buildings*, Washington, DC, USA, 1996.

[5] D.O.E., *Technical Installation Review, December 1997: WhiteCap Roof Spray Cooling System*, U.S. Department of Energy, 1997.

[6] Y. Man, H. Yang, J. D. Spitler, and Z. Fang, "Feasibility study on novel hybrid ground coupled heat pump system with nocturnal cooling radiator for cooling load dominated buildings," *Applied Energy*, vol. 88, no. 11, pp. 4160–4171, 2011.

[7] G. Heidarinejad, M. Farmahini Farahani, and S. Delfani, "Investigation of a hybrid system of nocturnal radiative cooling and direct evaporative cooling," *Building and Environment*, vol. 45, no. 6, pp. 1521–1528, 2010.

[8] M. Farmahini Farahani, G. Heidarinejad, and S. Delfani, "A two-stage system of nocturnal radiative and indirect evaporative cooling for conditions in Tehran," *Energy and Buildings*, vol. 42, no. 11, pp. 2131–2138, 2010.

[9] A. Y. T. Al-Zubaydi, J. Dartnall, and A. Dowd, "Design, construction and calibration of an instrument for measuring the production of chilled water by the combined effects of evaporation and night sky radiation," in *Proceedings of the International Mechanical Engineering Conference and Exposition (IMECE '12)*, Houston, Tex, USA, 2012.

[10] S. A. Klein, W. A. Beckman, J. W. Mitchell, and J. A. Duffie, *TRNSYS 16—A Transient System Simulation Program, User Manual*, Solar Energy Laboratory, University of Wisconsin, Madison, Wis, USA, 2004.

[11] P. Berdahl and M. Martin, "Emissivity of clear skies," *Solar Energy*, vol. 32, no. 5, pp. 663–664, 1984.

[12] R. W. Bliss Jr., "Atmospheric radiation near the surface of the ground: a summary for engineers," *Solar Energy*, vol. 5, no. 3, pp. 103–120, 1961.

[13] M. Martin and P. Berdahl, "Characteristics of infrared sky radiation in the United States," *Solar Energy*, vol. 33, no. 3-4, pp. 321–336, 1984.

[14] D. K. Kondepudi, *Introduction to Modern Thermodynamics*, John Wiley & Sons, New York, NY, USA, 1st edition, 2008.

[15] W. E. Ranz and W. R. Marshal, "Evaporation from drops—part II," *Chemical Engineering Program*, vol. 48, pp. 173–180, 1952.

[16] D. K. Kondepudi, *Introduction to Modern Thermodynamics*, John Wiley & Sons, New York, NY, USA, 2008.

[17] P. F. Incropera and P. D. DeWitt, *Fundamentals of Heat and Mass Transfer*, John Wiley & Sons, Hoboken, NJ, USA, 5th edition, 2002.

[18] A. M. Al-Turki and G. M. Zaki, "Energy saving through intermittent evaporative roof cooling," *Energy and Buildings*, vol. 17, no. 1, pp. 35–42, 1991.

[19] S. S. Kachhwaha, P. L. Dhar, and S. R. Kale, "Experimental studies and numerical simulation of evaporative cooling of air with a water spray—I. Horizontal parallel flow," *International Journal of Heat and Mass Transfer*, vol. 41, no. 2, pp. 447–464, 1998.

[20] P. Gandhidasan, "Simplified model for the behaviour of a roof-spray cooling system," *Applied Energy*, vol. 34, no. 1, pp. 69–77, 1989.

[21] S. N. Kondepudi, "A simplified analytical method to evaluate the effects of roof spray evaporative cooling," *Energy Conversion and Management*, vol. 34, no. 1, pp. 7–16, 1993.

[22] M. S. Sodha, U. Singh, A. Srivastava, and G. N. Tiwari, "Experimental validation of thermal model of open roof pond," *Building and Environment*, vol. 16, no. 2, pp. 93–98, 1981.